PERSONALIZED ANKLE - FOOT ORTHOSES FABRICATION VIA ADDITIVE MANUFACTURING AND DESIGN OF EXPERIMENT

CHẾ TẠO NẸP CHỈNH HÌNH MẮT CÁ CHÂN CÁ NHÂN HÓA THÔNG QUA PHƯƠNG PHÁP SẢN XUẤT BỒI ĐẮP VÀ THIẾT KẾ THÍ NGHIỆM

Le Hong Hieu[1], Giang Thi Kim Lien[2], Bui Quoc Huy Nguyen[2]*

[1]HUTECH Institute of Engineering, HUTECH University, Ho Chi Minh city, Vietnam
[2]The University of Danang - VNUK Institute for Research and Executive Education, Vietnam

*Corresponding author: huy.nguyenbuiquoc@vnuk.udn.vn

(Received: April 04, 2025; Revised: May 15, 2025; Accepted: May 27, 2025)

DOI: 10.31130/ud-jst.2025.23(7).187

Abstract - Ankle foot orthoses (AFOs) assist patients with foot lifting or stabilization difficulties caused by muscle weakness, nerve damage, or joint instability. Traditional fabrication methods, like plaster casting, are labor - intensive and time - consuming. 3D scanning and printing techniques offer a promising alternative, with quick and precise scanning and rapid fabrication. However, optimizing parameters for additive manufacturing remains challenging. This study uses a Taguchi - based design of experiment method to assess the impact of various 3D printing factors on the tensile strength of fabricated PP tensile specimens. The optimised parameters are the nozzle temperature of 240°C, the bed temperature of 60°C, the print speed of 15mm/s and the layer height of 0.1mm. Using measured mechanical properties of these specimens, a custom AFO design is evaluated via finite element analysis in ANSYS to assess mechanical behavior. This approach proves effective in evaluating and optimizing AFO fabrication, saving material, and reducing the number of experiments conducted.

Key words - Ankle foot orthosis; Additive manufacturing; Finite element analysis; Taguchi; Design of experiment.

Tóm tắt - Nẹp chỉnh hình mắt cá chân (AFO) hỗ trợ bệnh nhân gặp khó khăn khi nâng hoặc cố định bàn chân do yếu cơ, tổn thương thần kinh hoặc mất ổn định khớp. Phương pháp chế tạo AFO truyền thống, như đúc thạch cao, tốn công sức và thời gian. Kỹ thuật quét và in 3D là giải pháp thay thế hứa hẹn, với khả năng quét và chế tạo nhanh chóng. Tuy nhiên, việc tối ưu hóa yếu tố thiết kế vẫn còn nhiều thách thức. Nghiên cứu này dùng phương pháp thiết kế thí nghiệm Taguchi để đánh giá ảnh hưởng của các yếu tố in 3D đến độ bền kéo của mẫu nhựa PP được tạo ra. Thiết kế AFO tùy chỉnh được đánh giá qua phân tích phần tử hữu hạn trong ANSYS. Tham số tối ưu được xác định là nhiệt độ vòi phun là 240°C, nhiệt độ đế in là 60°C, tốc độ in là 15 mm/giây và độ dày lớp là 0,1 mm. Phương pháp này chứng minh hiệu quả trong việc đánh giá và tối ưu hóa AFO qua tiết kiệm vật liệu và giảm số lượng thí nghiệm cần tiến hành.

Từ khóa - Nẹp chỉnh hình mắt cá chân; Sản xuất bồi đắp; Phân tích phần tử hữu hạn; Taguchi; Thiết kế thí nghiệm.

1. Introduction

An ankle - foot orthosis (AFO) is an essential assistive device designed to improve mobility [1], [2]. AFO is commonly used for patients who have difficulty lifting or stabilizing the foot due to conditions such as muscle weakness, nerve damage, or joint instability [3]. During a standard gait cycle, these issues often lead to abnormal walking patterns, such as improper foot placement, increased foot pressure, excessive knee flexion, or high - stepping gait [4]. AFO typically has an "L" shape, with the vertical section resting behind the calf and the horizontal section positioned under the foot. This design helps improve foot movement and enhances walking safety. There are two main types of AFO: prefabricated and custom - made [5], [6]. A prefabricated AFO is mass - produced in fixed sizes and cannot be customized. However, due to the diversity in foot and lower limb sizes among patients, a prefabricated AFO often does not meet practical needs. Therefore, a custom - made AFO, which is specifically designed according to the individual requirements of each patient, becomes a more effective solution to ensure proper fit and to meet personal mobility demands.

Although both additive manufacturing (AM) and conventional manufacturing (CM) can produce a custom - made AFO that meets criteria for lightweight, fit, durability, and reasonable cost, AM offers significant advantages. Compared to AM, CM involves multiple complex manual steps, from plaster casting of the patient's lower leg, to creating negative and positive molds for shaping thermoplastic sheets, and finally producing the orthosis in the desired form [8]. However, this process requires high manual skill and is time - consuming. In contrast, AM uses a 3D scanner to quickly capture the shape of the leg directly, eliminating the plaster casting and mold adjustment steps, and significantly reducing production time - from several days with CM to just a few hours [3], [9]. 3D printing technology also allows for easy design modification of the orthosis through computer - aided design (CAD) software, saving material and minimizing the risk of manual errors [10]. Furthermore, the absence of plaster reduces environmental impact by limiting landfill waste or the need for thermal recycling [11].

However, when applying AM to fabricate an orthosis, the quality of the printed product remains a critical concern. A 3D - printed orthosis must not only ensure

comfort for the wearer but also achieve mechanical properties such as high tensile strength to guarantee safety during use [12], [13]. These properties depend on the manufacturing parameters and the printing materials used. To optimize the fabrication process, the Taguchi design of experiments (DoE) method is applied, instead of the traditional full factorial approach which requires a large number of experiments [14], [15].

In this study, 3D - printed polypropylene (PP) tensile specimens were fabricated with various combinations of printing parameters to determine the mechanical properties of the printed material. The Taguchi DoE method was applied to optimize the printing parameters, including nozzle temperature, bed temperature, print speed, and layer thickness, to achieve the desired mechanical properties. In addition, 3D surface data obtained from a volunteer's lower leg were used as digital input for designing the AFO in CAD software. The orthosis design was then refined based on the 3D scan data and evaluated using finite element analysis (FEA) in Ansys. The finalized AFO design file was then exported to a 3D printer for fabrication using the optimized parameters. To the best of our knowledge, this is the first study to integrate DoE methodology, statistical analysis, and FEA to optimize and fabricate a custom - made AFO using 3D printing technology. This approach promises to enhance design flexibility, optimize costs, and increase practical applicability, while ensuring high quality for the fabricated AFO.

2. Materials and methods

2.1. Materials

A 1.75 mm diameter PP filament used for 3D printing was supplied by YOUSO, China.

2.2. Equipment

PP tensile specimens and the orthosis were printed using a 3D printer (A8S, JGMaker, China). Printer settings were adjusted using UltiMaker Cura 5.6.0 software. Tensile tests were conducted on a 5 kN universal testing machine (Model 3365, INSTRON, USA). The shape of the lower leg was captured using a 3D scanner (Einscan Pro 2X, SHINING 3D Tech Co., Ltd., China).

3. Methods

3.1. Taguchi Design of Experiment (DoE) Method

The Taguchi method provides a solution for determining optimal factors by using an orthogonal array that contains a reasonable number of required experiments without compromising result reliability [16]. In this study, three different values were examined for each of four parameters, resulting in an L9 orthogonal array with 4 factors and 3 levels - a reasonable number of experiments compared to the 81 required for a full factorial design [17]. Table 1 outlines the investigated factors and their corresponding levels. Nozzle temperature values were selected based on the melting temperature of PP, which ranges from 200 - 250°C [18]. Printing factors kept constant throughout the experiment included nozzle diameter at 0.4 mm, infill density at 100%, and grid infill pattern for all printed specimens and the orthosis. All layer thicknesses were selected according to the printer's specifications, with allowable values from 0.05 to 0.3 mm.

To assess the effect of printing parameters on tensile strength, the "higher - the - better" signal - to - noise ratio (SNR) was applied, since the aim was to maximize tensile strength for both specimens and the orthosis. The corresponding SNR formula is:

$$SNR = -10log_{10}\left(\frac{1}{n}\sum_{i=1}^{n}\frac{1}{y_i^2}\right) \quad (1)$$

Where, y_i and n are the observed value for the i - th trial and the number of observations, respectively [19]. Table 2 lists the printing factors and their levels, the measured tensile strength for each trial, the corresponding mean values, and their SNRs.

Table 1. *List of control factors and their corresponding levels*

No.	Factor	Unit	Level		
			1	2	3
1	Nozzle Temperature	°C	200	220	240
2	Heated Bed Temperature	°C	60	70	80
3	Print Speed	mm/s	10	15	20
4	Layer Thickness	mm	0.1	0.15	0.2

3.2. Specimen preparation and tensile testing

Tensile specimens were printed according to the American Society for Testing and Materials (ASTM) D638 Type I standard [20]. Tensile tests were performed at a crosshead speed of 100 mm/min. Young's modulus and tensile strength were calculated from the stress - strain curve. To ensure repeatability, each trial was conducted using three specimens, and the average value was calculated.

3.3. 3D leg scanning and orthosis design

A handheld scanner was used in this step, with the patient's leg held in a relaxed position. The technician maintained a distance of less than 400 mm from the leg and moved the scanner around it to collect data. The entire scanning process took approximately 2 to 3 minutes.

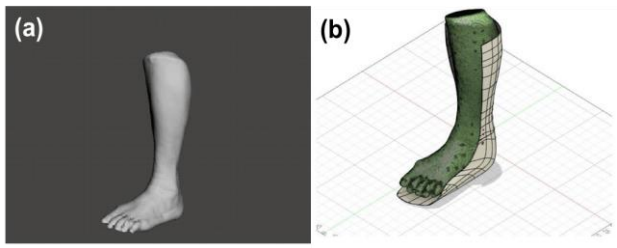

Figure 1. *(a) 3D model of scanned leg in Meshmixer and (b) AFO design based on the scanned 3D model*

3.4. AFO design

The obtained 3D foot model in STL format was imported into Meshmixer software for further editing of irregularities or errors, as shown in Figure 1(a). Once a suitable model was achieved, the leg model was saved in STL format for import into Autodesk Fusion 360. Using the Form tool in Fusion's workspace, the AFO design was created to match the shape and size of the leg (Figure 1(b)).

3.5. Finite element analysis (FEA) for orthosis design evaluation

The orthosis design model was analyzed to determine deformation and maximum stress for different material

properties and boundary conditions. In this study, the scenario considered was when the foot is in full contact with the ground during each step or while standing. In Figure 2(a), the three - point force principle applied in the AFO design is illustrated, with F1 as the main force and F2 and F3 as the reaction forces applied above and below the main force. The three - point force model helps address deformations such as excessive tilt and valgus angles. By restricting movement around the joint axis, this system allows for control of rotational movement and provides joint stability [21], [22]. The applied force values for F1, F2, and F3 were 60.1 N at the heel, 42.7 N at the proximal posterior calf, and 23.8 N at the dorsum of the foot, respectively [23]. Figure 2(b) shows the mesh model of the AFO, where the mesh size is 6 mm, with about 19,500 nodes and over 3,600 elements.

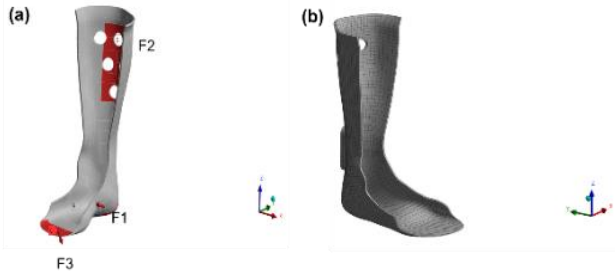

Figure 2. *(a) Force diagram and (b) the AFO mesh*

4. Results and discussion

4.1. Optimization of 3D printing parameters using the Taguchi method

Table 2. *Experimental results presented by L9 orthogonal array*

No.	Nozzle Temperature (°C)	Bed Temperature (°C)	Print Speed (mm/s)	Layer Thickness (mm)	Tensile strength (MPa)	SNR
1	200	60	10	0.1	27; 27,1; 27,2	28.659
2	200	70	15	0.15	26; 26,1; 26,2	28.333
3	200	80	20	0.2	25,2; 25,3; 25,4	28.062
4	220	60	15	0.2	27,6; 27,7; 27,8	28.849
5	220	70	20	0.1	28,3; 28,4; 28,5	29.066
6	220	80	10	0.15	26,9; 27; 27,1	28.627
7	240	60	20	0.15	28,8; 28,9; 29	29.218
8	240	70	10	0.2	28,2; 28,3; 28,4	29.036
9	240	80	15	0.1	29,1; 29,2; 29,3	29.308

Representative stress - strain curves for the specimen with the lowest tensile strength (experiment number 3) and the highest (experiment number run 9) are shown in Figure S1. From Table 2, the graphs depicting the mean SNR values corresponding to each level of the printing factors are shown in Figure 3, and the mean SNR values are summarized in Table 3.

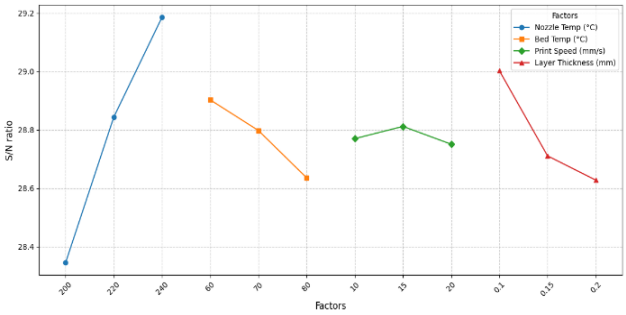

Figure 3. *The SNR of four printing factors*

Table 3. *Mean SNR by levels*

Level	Nozzle Temperature (°C)	Bed Temperature (°C)	Print Speed (mm/s)	Layer Thickness (mm)
1	28.345	28.903	28.77	29.003
2	28.844	28.798	28.812	28.711
3	29.186	28.636	28.751	28.628
Difference	0.841	0.267	0.061	0.375
Rank	1	3	4	2

Analysis of variance (ANOVA) was performed to determine experimental error and to identify which factors significantly affected the results. The results are presented in Table 4.

Table 4. *ANOVA results of four factors*

Factor	DOF	SS	MS	F - value	P	% Contribution
Nozzle Temperature (°C)	2	31.4867	15.7433	1574.33	0.000	77.27%
Heated Bed Temperature (°C)	2	2.4467	1.2233	122.33	0.000	6.00%
Print Speed (mm/s)	2	0.1867	0.0933	9.33	0.002	0.46%
Layer Thickness (mm)	2	6.4467	3.2233	322.33	0.000	15.82%
Error	18	0.18	0.01			0.44%
Total						100%

Among the four printing parameters, nozzle temperature had the greatest impact, contributing 77.27% of the variation, with a statistically significant P - value (0.000) and the highest F - value (1574.33). The second most influential factor was layer thickness, contributing 15.82%. Print speed and bed temperature contributed only marginally to the experimental variance. The error accounted for only 0.44% of the total variation, indicating that the experimental process was well controlled with minimal unexplained variance.

In summary, nozzle temperature and layer thickness should be prioritized for optimizing the printing process, while print speed and bed temperature, though less important, should still be controlled to ensure stability. These ANOVA results are consistent with the range values and the order of influence of each factor on tensile strength as previously shown in Table 3.

Based on the optimal combination of printing parameters, a tenth set of specimens was fabricated and tensile tests were conducted to determine the mechanical properties for Ansys simulation input. The tensile specimens were fabricated using the optimal 3D printing parameters: nozzle temperature of 240°C, bed temperature of 60°C, print speed of 15 mm/s, and layer thickness of 0.1 mm. The results showed a tensile strength of 28 ± 0.6 MPa and a Young's modulus of 2000 ± 15 MPa.

4.2. FEA Simulation results

To estimate the stiffness of the designed AFO model, Ansys simulation results are shown in Figure 4. The region of maximum total displacement was observed around the toe area (Figure 4(a)). The maximum stress values occurred around the medial and lateral edges of the AFO, which are also the joints of the AFO. The highest strain was clearly located at the points of maximum stress, as illustrated in Figure 4(b,c).

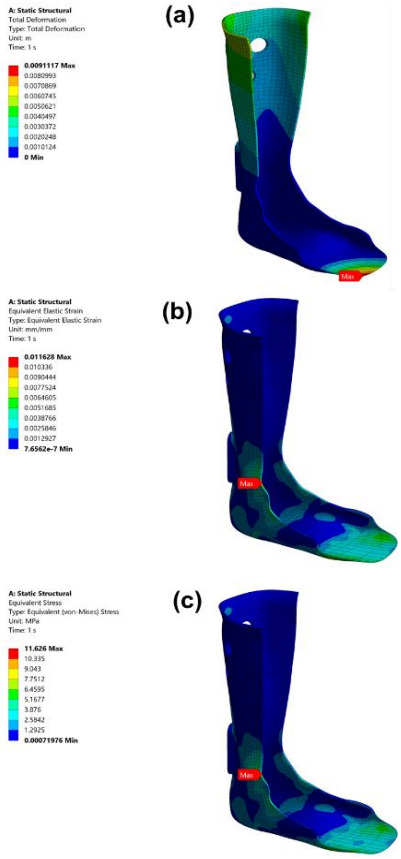

Figure 4. *Ansys simulation results of (a) total deformation, (b) strain and (c) stress of the designed AFO*

4.3. 3D Printing of the orthosis

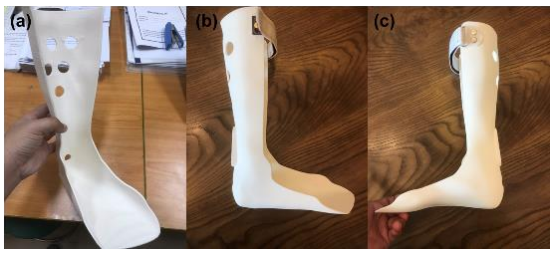

Figure 5. *Printed AFO with (a) front view, (b) right lateral view, and (c) left lateral view*

Figure 5 illustrates the AFO printed using the optimized set of 3D printing parameters described above.

5. Conclusion

In summary, this study successfully demonstrated a comprehensive approach for 3D printing polypropylene (PP) specimens and custom AFO design. By employing the Taguchi design of experiments method, the optimal combination of 3D printing parameters - nozzle temperature of 240°C, bed temperature of 60°C, print speed of 15 mm/s, and layer thickness of 0.1 mm - was identified to achieve the desired mechanical properties. This optimal printing combination was used to fabricate a set of specimens, whose mechanical properties served as input for FEA simulation of the AFO. Using 3D surface data from the patient's foot, the AFO was designed in CAD software and its mechanical behavior was evaluated through FEA in ANSYS. This study represents the first integration of experimental, statistical, and FEA approaches for producing a custom 3D - printed AFO. The proposed method has significant potential for enhancing design flexibility, cost - effectiveness, and service capacity, while ensuring high quality of the custom AFO.

Acknowledgments: This work was supported by The University of Danang – VN-UK Institute for Research and Executive Education, under project code: T2024 - VNUK - 02.

REFERENCES

[1] E. Wojciechowski *et al.*, "Feasibility of designing, manufacturing and delivering 3D printed ankle - foot orthoses: A systematic review", *J Foot Ankle Res,* vol. 12, no. 11, 2019, doi: 10.1186/s13047 - 019 - 0321 - 6.

[2] M. Taghavi, T. Helps, B. Huang, and J. Rossiter, "3D - Printed Ready - To - Use Variable - Stiffness Structures", *IEEE Robot Autom Lett*, vol. 3, no. 3, 2018, doi: 10.1109/LRA.2018.2812917.

[3] A. Nouri, L. Wang, Y. Li, and C. Wen, "Materials and Manufacturing for Ankle - Foot Orthoses: A Review", *Adv. Eng. Mater*., vol. 25, no. 20, 2300238, 2023. doi: 10.1002/adem.202300238.

[4] L. Everaert, E. Papageorgiou, A. Van Campenhout, L. Labey, and K. Desloovere, "The influence of ankle - foot orthoses on gait pathology in children with cerebral palsy: A retrospective study", *Gait Posture*, vol. 100, 2023, doi: 10.1016/j.gaitpost.2022.11.063.

[5] M. H. Ali, Z. Smagulov, and T. Otepbergenov, "Finite element analysis of the CFRP - based 3D printed ankle - foot orthosis", *Procedia Computer Science*, vol. 179, pp. 55 - 62, 2021. doi: 10.1016/j.procs.2020.12.008.

[6] Y. J. Choo and M. C. Chang, "Commonly used types and recent development of ankle-foot orthosis: A narrative review", *Healthcare (Basel)*, vol. 9, no. 8, 1046, 2021. doi: 10.3390/healthcare9081046.

[7] M. Hamedi, P. Salimi, A. Aliabadi, and M. Vismeh, 'Toward intelligent ankle foot orthosis for foot - drop, a review of technologies and possibilities', in *Proceedings - 2015 2nd International Conference on Biomedical Engineering, ICoBE 2015*, 2015. doi: 10.1109/ICoBE.2015.7235875.

[8] A. Cieza *et al.*, *Standards for Prosthetics and Orthotics,* Part 1: Standars. World Health Organization & USAID, 2017.

[9] M. Farhan, J. Z. Wang, P. Bray, J. Burns, and T. L. Cheng, "Comparison of 3D scanning versus traditional methods of capturing foot and ankle morphology for the fabrication of orthoses: a systematic review", *Foot Ankle Res*, vol. 14, no. 2, 2021. doi: 10.1186/s13047 - 020 - 00442 - 8.

[10] B. R. Hunde and A. D. Woldeyohannes, "Future prospects of computer - aided design (CAD) - A review from the perspective of artificial intelligence (AI), extended reality, and 3D printing", *Results Eng.*, vol. 14, 2022. doi: 10.1016/j.rineng.2022.100478.

[11] R. H. Geraldo *et al.*, "Gypsum plaster waste recycling: A potential environmental and industrial solution", *J Clean Prod*, vol. 164, 2017, doi: 10.1016/j.jclepro.2017.06.188.

[12] C. H. Yeh, K. R. Lin, F. C. Su, H. Y. Hsu, L. C. Kuo, and C. C. Lin, "Optimizing 3D printed ankle - foot orthoses for patients with stroke: Importance of effective elastic modulus and finite element simulation", *Heliyon*, vol. 10, no. 5, 2024, doi: 10.1016/j.heliyon.2024.e26926.

[13] R. Raj *et al.*, "Numerical and Experimental Mechanical Analysis of Additively Manufactured Ankle - Foot Orthoses", *Materials*, vol. 15, no. 17, 2022, doi: 10.3390/ma15176130.

[14] W. H. Chen *et al.*, "A comprehensive review of thermoelectric generation optimization by statistical approach: Taguchi method, analysis of variance (ANOVA), and response surface methodology (RSM)", *Renewable Sustainable Energy Rev.,* vol. 169, 112917, 2022. doi: 10.1016/j.rser.2022.112917.

[15] G. Mounika, K. Rajyalakshmi, G. V. S. Rajkumar, and D. Sravani, "Prediction and optimization of process parameters using design of experiments and fuzzy logic", *International Journal on Interactive Design and Manufacturing*, vol. 18, no. 4, 2024, doi: 10.1007/s12008 - 023 - 01446 - x.

[16] B. Maazinejad *et al.*, "Taguchi L9 (34) orthogonal array study based on methylene blue removal by single - walled carbon nanotubes - amine: Adsorption optimization using the experimental design method, kinetics, equilibrium and thermodynamics", *J Mol Liq*, vol. 298, 2020, doi: 10.1016/j.molliq.2019.112001.

[17] J. A. Afonso, J. L. Alves, G. Caldas, B. P. Gouveia, L. Santana, and J. Belinha, "Influence of 3D printing process parameters on the mechanical properties and mass of PLA parts and predictive models", *Rapid Prototyp J*, vol. 27, no. 3, 2021, doi: 10.1108/RPJ - 03 - 2020 - 0043.

[18] L. Wang, J. E. Sanders, D. J. Gardner, and Y. Han, "Effect of fused deposition modeling process parameters on the mechanical properties of a filled polypropylene", *Progress in Additive Manufacturing*, vol. 3, no. 4, 2018, doi: 10.1007/s40964 - 018 - 0053 - 3.

[19] P. Sharma, M. Sivaramakrishnaiah, B. Deepanraj, R. Saravanan, and M. V. Reddy, "A novel optimization approach for biohydrogen production using algal biomass", *Int J Hydrogen Energy*, vol. 52, 2024, doi: 10.1016/j.ijhydene.2022.09.274.

[20] F. H. Abdalsadah, F. Hasan, Q. Murtaza, and A. A. Khan, "Design and Manufacture of a custom ankle - foot orthoses using traditional manufacturing and fused deposition modeling", *Progress in Additive Manufacturing*, vol. 6, no. 3, 2021, doi: 10.1007/s40964 - 021 - 00178 - 2.

[21] K. Wang, P. Han, T. Ning, C. Yan, F. Li, and L. Wang, "An exploration into the orthopedic effect and patterns of the correction based on the three - point force system in patients with strephenopodia", *Foot & Ankle Surgery: Techniques, Reports & Cases*, vol. 4, no. 1, 2024, doi: 10.1016/j.fastrc.2023.100355.

[22] C. F. Hovorka, G. F. Kogler, Y. H. Chang, and R. Gregor, "Material properties and application of biomechanical principles provide significant motion control performance in experimental ankle foot orthosis - footwear combination", *Clinical Biomechanics*, vol. 82, 2021, doi: 10.1016/j.clinbiomech.2021.105285.

[23] M. A. Arnold, "*Finite element analysis of ankle foot orthoses"*, Ph.D. dissertation, Faculty of Engineering and Applied Science, Department of Mechanical Engineering, University of Southampton, 1999. https://eprints.soton.ac.uk/393597/

APPENDIX

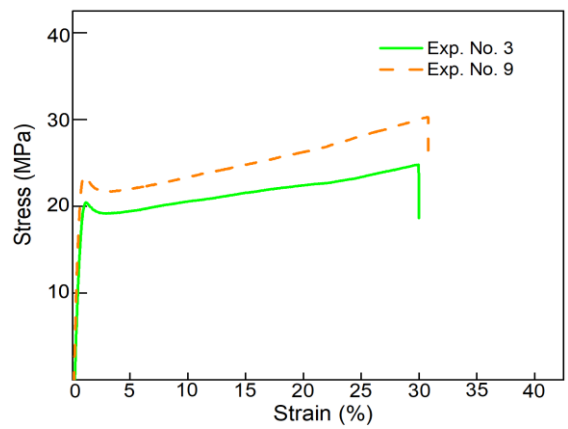

Figure S1. *Stress - strain curves of experiment number 3 (green solid line) and experiment number 9 (orange dashed line)*